Experimental Characterisation of the Off-Body Wireless Channel at 2.4 GHz for Dairy Cows in Barns and Pastures

Said Benaissa [a, b,*], David Plets[a], Emmeric Tanghe[a], Leen Verloock[a], Luc Martens[a], Jeroen Hoebeke[a], Bart Sonck[b,c], Frank André Maurice Tuyttens [b], Leen Vandaele[b], Nobby Stevens[d], Wout Joseph[a]

[a] Department of Information Technology, Ghent University/iMinds, Gaston Crommenlaan 8 Box 201, B-9050 Ghent, Belgium

[b] Institute for Agricultural and Fisheries Research (ILVO)-Animal Sciences Unit, Scheldeweg 68, 9090 Melle, Belgium

[c] Department of Biosystems Engineering, Faculty of Bioscience Engineering, Ghent University, Coupure links 653, B-9000 Ghent, Belgium

[d] DraMCo research group, ESAT, Faculty of Engineering Technology, KU Leuven, Gebroeders De Smetstraat 1, 9000 Ghent, Belgium

*** Corresponding author. Tel.: +32 09 331 48 99; fax: +32 09 331 48 99 E-mail address: said.benaissa@intec.ugent.be (S. BENAISSA)**

Abstract

Wireless Sensor Networks (WSNs) provide promising applications in healthcare monitoring of dairy cows. After sensors measure the data in or on the cow's body (temperature, position, leg movement), this information needs to be transmitted to the farm manager, enabling the evaluation of the health state of the cow. In this work, the off-body wireless channel between a node placed on the cow's body and an access point positioned in the surroundings of the cows is characterised at 2.4 GHz. This characterisation is of critical importance in the design of reliable WSNs operating in the industrial, scientific and medical (ISM) band (e.g., Wi-Fi, ZigBee, and Bluetooth). Two propagation environments were investigated: indoor (inside three barns) and outdoor (pasture). Large-scale fading, cow body shadowing, and temporal fading measurements were determined using ZigBee motes and spectrum analysis measurement. The path loss was well fitted by a one-slope log-normal model, the cow body shadowing values increased when the height of the transmitter and/or the receiver decreased, with a maximum value of 7 dB, and the temporal fading due to the cow movement was well described by a Rician distribution in the considered environments. As an application, a network planning tool was

used to optimise the number of access points, their locations, and their power inside the investigated barns based on the obtained off-body wireless channel characteristics. Power consumption analysis of the on-cow node was performed to estimate its battery lifetime, which is a key factor for successful WSN deployment.

Keywords

Wireless sensor network (WSN), off-body communication, propagation, large-scale fading, temporal fading, network planning.

1. Introduction

With the advances in wireless communication and micro-electro-mechanical systems (MEMS) (Kahn et al., 2000), computing devices have become smaller, cheaper, combined with an increased functionality and a higher energy efficiency. This technological evolution has enabled the establishment of Wireless Sensor Networks (WSNs). A WSN is a collection of sensing devices where each node can sense, process, save and exchange data wirelessly through a network. WSNs are finding various applications in areas of medicine, agriculture, sports and multimedia (Akyildiz et al., 2002; Alemdar and Ersoy, 2010).

WSNs can be effectively used in health tracking of dairy cows to facilitate herd management and cow welfare. They can be used for detecting diseases such as lameness and mastitis, which are considered as the majors health problems in dairy farming (Barkema et al., 1994). Extensive studies on cattle health monitoring with WSNs were already published (Andonovic et al., 2010; Mayer et al., 2004; Nadimi et al., 2008; Wietrzyk and Radenkovic, 2010). In (Nadimi et al., 2012), authors used a ZigBee-based mobile ad hoc WSN to monitor and classify animal behaviour (e.g. grazing, lying down, walking and standing), which provides reliable information about animal health and welfare. Another study (Huircán et al., 2010) proposed a localisation scheme for cattle monitoring applications in grazing fields using a ZigBee-based WSN. Kwong et al., 2012 presented practical considerations that are faced by WSNs for cattle monitoring such as deployment challenges (e.g., mobility, radio interference caused by the animals and limitations in data storage of the devices), design consideration (changes of network topology due to the constant movement of the herd) and wireless communication issues (signal penetration depth through an animal body, height optimisation of the collar and access point antennas, bandwidth, data load, and power consumption). However, none of these studies has presented detailed models describing the radio propagation channel required for a WSN deployment in an indoor (barn) or outdoor (pasture) environment.

When the sensors receive health parameters from the cow's body (e.g., temperature, position, leg movement), this information should be forwarded to a back-end access point placed in the proximity of the cows. Next, these data are transferred to a central data processing server. Finally, the farm manager can decide on the health state of each individual cow in an early stage by analysing the received alert or warnings messages. The communication between the on-cow node and the back-end access point inside the barn or on the pasture will be susceptible to frequent signal blocking events caused by the cow wearing the node and the other cows in the vicinity of the transmitter. The reliability of this off-body wireless communication is a crucial parameter for the success of healthcare monitoring systems. The characterisation of the physical layer, including an estimation of the path loss between nodes placed on the cow body and the access point, is an important step in the realisation of reliable off-body communication. To the best of our knowledge, no work has addressed the characterisation of such off-body wireless links in barns and pastures of dairy cows.

The novelties of this paper are the following: (i) Determination of the off-body path loss in indoor (three different barns) and outdoor (pasture) environments using ZigBee motes and spectrum analysis equipment, (ii) Estimation of the cow body shadowing, (iii) Temporal fading measurements to characterise the time variation of the wireless channel, (iv) Barn and pasture wireless network planning for healthcare monitoring of dairy cows.

The remainder of the paper is structured as follows. Section 2 describes the methods that have been used to characterise the wireless channel. In Section 3, the measurement methodology is presented.

Section 3.1 presents the measurement environments, while Section 3.2 explains the measurement setup in both indoor and outdoor environments. Then in Section 4, the obtained results are presented and discussed. These results are used for the network planning performed in Section 5. Finally, conclusions are drawn and future work is discussed in Section 6.

2. Methods

2.1 Characterisation of large-scale fading

In wireless communication, the fading phenomenon denotes the variation of the received power in a certain propagation environment. The fading may vary with time, position orientation or frequency. The characterisation of the fading requires accurate analysis of the received power. The received signal envelope comprises a small-scale fading component superimposed on a large-scale fading part (Lee, 1985). The terms small and large here are used in comparison to the wavelength. Since, the large-scale fading is defined as the variability of received power over distance intervals of a few wavelengths, estimating the large-scale fading from the received signal is the same as obtaining the local averaged power over few wavelengths of it (Lee, 1985).

After estimating a local average received power for each transmitter-receiver constellation, the path loss should be calculated and modelled. The path loss model can be used in the link budget calculation and network planning for wireless monitoring and communication in barns and pastures. From the measured average received power P_{RX} (measured by a spectrum analyser), the path loss $PL(dB)$ is calculated as follows:

$$PL = P_{TX} + G_{TX} - L_{TX} + G_{RX} - L_{RX} - P_{RX} \quad (1)$$

where P_{TX} is the transmitter power (dBm), G_{TX} the transmitter antenna gain (dBi), L_{RX} the transmitter cable losses (dB), G_{RX} the receiver antenna gain (dBi) and L_{RX} the receiver cable losses (dB).

In general, the large scale variations of the path loss around the median as a function of the distance tend to have a Gaussian distribution (in dB) or a lognormal distribution (when expressed linearly)

(Pérez Fontán and Mariño Espiñeira, 2008; Tanghe et al., 2008). Here, a one-slope path loss model is used to fit the measured values using the equation (Rappaport, 2002):

$$PL(d) = PL(d_0) + 10n \log\left(\frac{d}{d_0}\right) + X_\sigma \quad (2)$$

with $PL(d_0)$ is the path loss at reference distance $d_0 = 1$ m , n the path loss exponent, d the separation distance between TX and RX, and X_σ a zero-mean Gaussian distributed variable (in dB) with standard deviation σ, also in dB. $PL(d_0)$ and n are obtained from the measured data by the method of linear regression (LR) analysis. The path loss models can then be used in network planning to design WSNs for barns and pastures (Section 5).

2.2 Temporal fading statistics

In a typical wireless communication environment, often multiple propagation paths exist between the transmitter and the receiver. This multipath propagation phenomenon caused by the reflections, diffractions, and scattering of the signal by different objects, leads to different attenuations, distortions, delays and phase shifts. Temporal fading denotes the variability of the received power over time while the transmitter and the receiver remain at fixed locations in the propagation environment. This fading is mainly caused by the movement of objects between the transmitter and the receiver (e.g. cows, humans, materials), thereby influencing the propagation paths. In these conditions, communication can be difficult. Therefore, a fade margin should be considered in the design of a wireless communication system, to ensure a sufficiently high power reception during a certain percentage of the time. In many circumstances, it is too complicated to describe all the time variations that determine the different multipath components and the fade margin. Rather, this margin is determined by analysing the statistics of the fading. In non-line-of-sight (NLOS) conditions or where there is no dominant multipath component between the transmitter and the receiver, the probability density function (PDF) of the mean received signal amplitude follows a Rayleigh distribution. However, fading statistics follow a Ricean distribution when an undisturbed multipath component (e.g., LOS component) is present (Parsons, 2000). For the temporal variations of the received power, we expected a dominant multipath component between transmitter and receiver antenna. Therefore, the Rician distribution is adopted to characterise the temporal fading. This assumption is validated by comparing the theoretical Rice distributions to the measured temporal fading samples.

The Ricean distribution is often described in terms of a parameter K (Ricean factor), which is defined as the ratio between the power received via the dominant path and the power contribution of the obstructed paths (Abdi et al., 2001). The parameter K is given by $K = A^2/2b^2$ or in terms of dB:

$$K(dB) = 10 \log\left(\frac{A^2}{2b^2}\right) \tag{3}$$

In (3), A^2 is the energy of the dominant path and $2b^2$ is the energy of the diffuse part of the received signal (Bernadó et al., 2015). From the definition of the Rician K-factor, low K-factors indicates large motion (i.e., large b) within the wireless propagation environment that disturbs the received power profile over time, while large K-factors reveal a low movement in the environment. To estimate the K-factor, the method of moments proposed in (Abdi et al., 2001) was used. This method provides a simple parameter estimator based on the variance $V[R^2]$ and the mean $E[R^2]$of the received signal envelop square $(R(t))^2$. The Rician K-factor is given in (Abdi et al., 2001) by:

$$K = \frac{\sqrt{1-\gamma}}{1-\sqrt{1-\gamma}} \tag{4}$$

Where γ is defined as follows:

$$\gamma = V[R^2]/(E[R^2])^2 \tag{5}$$

3. Measurement Methodology

3.1 Measurement environments

Indoor measurements were carried out inside three barns. First, a modern barn of the Institute for Agricultural and Fisheries Research (ILVO), Melle, Belgium (Fig. 1-a) was considered. This barn, which houses approximately 144 lactating dairy cows, contains 2 milking robots, a conventional milking parlour, concentrate feeders and several features enabling experimental setups. Inside the barn, four similar areas are dedicated for cows lying down. These four areas have the same size and topology. Therefore, measurements were performed in one single area. Each area is about 29x9 m2 and of consists of 32 cubicles. Second, indoor measurements were conducted inside two other barns (UGent-Biocentrum Agrivet, Melle, Belgium) as shown in Fig. 1 (c) and (d). The dimensions of barns 2 and 3 were 42x26 m2 and 37x21.5 m2, respectively. As barn 1, barn 2 (Fig. 1-c) is dedicated for dairy cows and contains concentrate feeders and one milking robot. However, barn 3 (Fig. 1-d) is a new calf barn that can accommodate about 100 animals of different ages (from the first day until the age of two years when they calve for the first time). For each of these ages, appropriate boxes (individually or in groups on straw and slatted floor with mats and mattresses) are provided.

The second investigated off-body wireless communication environment was outdoor. Outdoor measurements were conducted in a pasture (Fig. 1-b) of about 33x15 m2 near the ILVO barn. All measurements were carried out in the 2.4 GHz band in three barns and a pasture. The 2.4 GHz band was selected because it is freely available and most practical existing technologies for WSNs work in this band.

3.2 Measurement setup

The physical modelling of the off-body wireless channel includes different parameters. In the present work, we focused on the following aspects. First, the large-scale fading due to the physical environment, which is characterised by the variation of the path loss with the distance. Then, the specific shadowing introduced by one cow's body. Finally, the variation of the wireless channel over time (i.e., temporal fading).

3.2.1 Large-scale fading measurements

To characterise the large-scale fading of the wireless channel, experiments were performed in both indoor (barns) and outdoor (pasture) environments. For each environment, two scenarios were performed, namely: without and with cows. In the first scenario, reference measurements were done in empty (without cows) barns and on an empty pasture. These experiments allowed a characterisation of the environments without the influence of the cows. Later, measurements with cows (second scenario) determined how much the random presence of the cows affects the wireless communication.

Fig. 2 shows the measurement equipment of the first scenario. The transmitter part (Fig. 2-a) consists of a transmitting antenna (TX) and a signal generator. As the TX, an omnidirectional vertically polarized antenna of type Jaybeam MA431Z00 (2.4 GHz, 4.2 dBi) was used. The TX antenna was mounted on a plastic mast with an adjustable height. The TX antenna was connected to the Rohde & Schwarz SMB100A (100 kHz - 12.75 GHz) signal generator used to inject a continuous wave signal at 2.4 GHz with a constant power of 18 dBm. The receiver part (Fig. 2-b) consists of a receiving antenna (Rx) mounted on a telescopic mast. At the Rx, an omnidirectional antenna of the same type as the TX was used. The Rx antenna was connected to a Rohde & Schwarz FSL6 (9 kHz - 6 GHz) spectrum analyser, which samples the received power level at the transmitting frequency. Sampled power values were stored on a laptop through a General Purpose Interface Bus (GPIB) connection. The spectrum analyser's frequency span was set to 100 kHz. The resolution and video bandwidth were set to 3 kHz and 30 kHz, respectively. According to (Tanghe et al., 2008), the resolution bandwidth has the largest effect on the measured power. However, the video bandwidth has a negligible effect. The use of a resolution bandwidth of 3 kHz is justified also in this paper by the small bandwidth of the continuous wave signal.

Fig. 1 shows the transmitter and the receiver locations inside the barns and on the pasture. In the first barn (Fig. 1-a), the receiver was fixed at the front right of the concerned area with an antenna height of 4.5 m, which is a typical height of the access points. Then, the position of the transmitter was set inside each box to a height h_{tx} of 0.9 m above the ground. This TX height is comparable to the height of a cow's neck. The width of each box is 1.15 m. Measurements were performed for a range of distances (TX-RX separation) between 7 m (nearest box) and 27 m (far box). The same TX and RX heights were considered for barns 2 and 3. Inside barn 2, measurement were performed for a range of distances between 4 m and 40 m. This range was 4 to 36 m for barn 3. For the outdoor measurements, the receiver was fixed at the corner of the pasture, also at a height of 4.5 m. Different positions of the transmitter were taken then as follows. The pasture was divided into three paths separated by a distance of 4 m. Each path was divided into different measurement locations with a separation of 2.5 m. Similarly to indoor environment, the height of the transmitter was set at 0.9 m. The range of distances between the transmitter and the receiver was 6 to 29 m.

At each measurement location (indoor and outdoor), 200 samples were recorded with a sampling rate of about 7 samples per second. The position of the transmitting antenna was changed a few wavelengths around each measurement location (about 10 wavelengths) to obtain an average received power.

In the second scenario, the signal generator was removed and one cow was wearing a ZigBee mote while fifteen other cows (indoor) and eight cows (outdoor) were moving freely inside the measurement area. The ZigBee mote was configured as a transmitter and it was attached to the collar around the cow's neck (See Fig. 3). The ZigBee mote antenna separation from the cow body was fixed to 5 cm. The ZigBee mote was attached to the collar because the data measured in different parts of the cow's body (e.g., leg, ear, udder) could be be gathered by a collector placed on the cow's neck, and then, transmitted to the base station. The same receiver as during the first scenario was used (MA431Z00 antenna connected to spectrum analyser). In addition, a second ZigBee mote was added at the same height and location as the receiving antenna. This ZigBee mote reports 150 Received Signal

Strength Indicator (RSSI) values for each measurement location by receiving the packets transmitted by the other mote. The transmitting ZigBee mote (TX) was an XBee S2 (XB24-Z7WIT-004) module with an omnidirectional monopole antenna (integrated whip, 1.5 dBi). The receiving ZigBee mote (RX) was a RM090 module with a PCB F-antenna (1 dBi). During all measurements, the antennas were vertically polarised. Fig. 3 shows an example of a measurement on the pasture. The spectrum analyser and the ZigBee mote (RX) receive in parallel the signal and packets sent by the ZigBee mote (TX). The cow wearing the ZigBee mote was placed at the same transmitter positions as for scenario 1.

3.2.2 Maximal cow body shadowing by other cows

In realistic cases, the communication between the on-cow device and the back-end access point will be susceptible to frequent signal blocking events not only caused by the body of the cow wearing the transmit node, but also by other cows, which can obscure the dominant signal path between the transmitter and the receiver. In wireless communications, this well-known phenomenon is referred to as body shadowing.

In order to quantify the impact of the cow body shadowing, a dairy cow was used and shadowing measurements were conducted in an area of about 12x6 m^2 inside the ILVO barn. As shown in Fig. 4, the dairy cow was standing between the transmitter and the receiver.

The distance between the transmitter and the receiver was set to 6.5 m. This distance is sufficient to be in the far-field conditions (Balanis, 2005). Then, different TX and RX antenna heights were investigated as shown in Fig. 4: 2 m and 4.5 m for the transmitter and 0.5 m, 1 m, 1.4 m, and 2 m for the receiver. The heights of the TX were chosen as the typical heights of the access point. However, the RX heights were chosen with respect to the cow's neck when the cow is standing, grazing, or lying down. Also, to account for just the cow body shadowing, measurements were performed first without cow.

3.2.3 Temporal fading

The temporal fading measurements were conducted in indoor and outdoor environments (barn 1 and pasture as described in Section 3.2.1) using the same equipment as in scenario 1 (see Fig. 2). However, the transmitter and receiver were set in stationary positions with a line of sight (LOS) condition at the beginning of the experiment. The antenna heights were $h_{tx} = 0.9\,m$ and $h_{rx} = 4.5\,m$. These scenarios were set to allow the recording of received signal power variations due to the movements of the cows. For both indoor and outdoor environments, received power was recorded during 20 min, including both LOS and Non-LOS (NLOS) conditions depending on the cows' movement. The received power was logged at a rate of approximately 20 samples per second. Thus, 24,000 received power samples were recorded in each environment.

3.3 RSSI calibration

The RSSI reported by the receiving ZigBee mote (off-cow) is just an indication (represented by a number) of the power level being received by the antenna. Thus, a calibration of the ZigBee mote using the spectrum analyser (SA) has been done to determine the shift constant between the RSSI and the radio-frequency (RF) power. For this aim, two experiments were performed as shown in Fig. 5.

In the first experiment (Fig. 5-a), a ZigBee mote was configured as a coordinator which constantly broadcasts packets (Transmitter). Then, two receivers were used to sense the received power. The first receiver was another ZigBee mote configured as a sniffer to capture broadcast signals (scenario 1 ZigBee-ZigBee). The second receiver comprised a spectrum analyser (R&S FSL6) connected to a MA431Z00 antenna (scenario 1 ZigBee-SA). The antenna and ZigBee motes were placed 1 m above the ground. The sniffer was used to avoid acknowledgment packets, which can affect the received power of the spectrum analyser. For different distances between the transmitter and the receivers, the RF power measured by the spectrum analyser and the RSSI reported by the ZigBee mote were logged using laptops.

In the second experiment (Fig. 5-b), the ZigBee motes were removed and the signal generator (SG) connected to the MA431Z00 antenna was used at the transmitter side. The same antenna type was used connected to the spectrum analyser (scenario 2 SG-SA). As in Section 3.2.1, the span of the spectrum analyser was set to 100 kHz. The resolution and video bandwidths were set to 3 kHz and 30 kHz, respectively. Exactly the same locations were measured as for the first experiment. In this way, the RSSI values reported by the ZigBee motes were calibrated with the SA equipment in actual power values (dBm or mW). In order to determine the relationship between the RSSI reported by the ZigBee mote and the RF power measured by the spectrum analyser, the path loss models of the calibration scenarios explained above were plotted in Fig 6, making use of equation (2). This figure shows that the path loss model (red line) obtained from the RSSI values reported by the ZigBee mote is 8 dB higher than the path loss model obtained from the received power of the spectrum analyser (dashed lines). Also, the path loss models signal generator- spectrum analyser (SG-SA) and ZigBee-spectrum analyser (ZigBee-SA) are perfectly matched.

Table 1 lists the parameter values of RSSI calibration path loss models. The path loss at the reference distance $PL(d_0 = 1\ m)$ was approximately the same (about 41 dB) for both scenarios ZigBee-SA and SG-SA. However, it shifted to 49 dB in the ZigBee-ZigBee scenario. The path loss exponents and the standard deviations were nearly the same for all scenarios. In conclusion, a constant shift of 8 dB will be considered between the $RSSI$ reported by ZigBee mote and the RF power P_{RF} (measured by the spectrum analyser as follows:

$$P_{RF}[dBm] = RSSI - 8\ dB \quad (6)$$

4. Results and discussion

4.1 Path loss models

4.1.1 Indoor path loss models

Fig. 7 shows the path loss values obtained by measurements and the fitted models versus log-distance (Tx-Rx separation) for the barns. The markers indicate the individual measurements, while the lines represent the path loss models obtained through fitting of the measurement data. As expected, the path loss inside the empty barns was lower than the path loss when the barn contains cows (3 dB). This is due to the cow's body shadowing (the cow wearing the mote and the other cows). Table 2 lists the parameter values of the obtained path loss models. The aim of the measurements performed inside the barns 2 and 3 was to validate the results of the barn 1. As shown in table 2, an excellent agreement between the path loss model parameters was obtained. Table 2 lists also the equivalent path loss model gathering the obtained data from all barns. All path loss exponents were lower than free space (n =2) due to the presence of multipath influence inside the barn. Similar path exponents were found by (Tanghe et al., 2008) in indoor industrial environments at 2.4 GHz. The standard deviations were 1.5 dB and 2.8 dB for the empty barns and barn with cows, respectively. This indicates a slightly higher degree of shadow fading due to the presence of cows inside the barn. The coefficient of determination R^2 measures how well the path loss model (regression line) approximates the real data points (measured path losses). It is defined as the square of the correlation between the measured and the predicted path losses (Wang et al., 2012). As shown in Table 2, coefficients of determination greater than 0.7 were obtained in both path loss models, indicating that the log-normal path loss model perfectly fits the measured data.

4.1.2 Outdoor path loss models

Path loss models for the pasture are shown in Fig. 8. The difference between the empty pasture and the pasture with cows is the same as the indoor (barns) case (3 dB). Table 3 lists the parameters of the path loss models obtained in the outdoor pasture environment. The path loss exponents are higher than for the barns (n =1.70) due to the rural environment (pasture), which is characterised by less influence of multipath components (less reflecting metal materials in comparison to the barns). The path loss difference between one cow and eight cows on the pasture is 0.5 dB (See Fig. 8). This means that the body of the cow wearing the node is the main reason of the path loss decrease. This is due to the high height of the base station (4.5 m), which makes the communication between the on-cow node and the base station either in LOS conditions or obscured just by the body of the cow wearing the node. Similar to the case of the indoor, the coefficients of determination (Table 3) of the outdoor are also greater than 0.7, meaning that the measured data is perfectly fitted by the predicted models.

To verify that the path loss variations indeed follow the log-normal distribution used to fit the measured path loss values, the predicted path loss is subtracted from the corresponding measured path loss samples. Then, this residual path loss is used as a parameter for the Quantile-Quantile (Q-Q) plot (Wilk and Gnanadesikan, 1968). Fig. 9 shows the Q-Q plot of residual path loss in indoor (barns) and outdoor (pasture) environments versus the standard Gaussian distribution. Fig. 9 aggregates all residuals path loss values of indoor scenarios (a) and outdoor scenarios (b). As shown in Fig. 9, the residual path loss matches well the Gaussian distribution, although there are some small deviations in the tails.

4.2 Cow body shadowing

The obtained values of the cow body shadowing for different TX and RX heights are listed in Table 4. The cow body shadowing varies from 1 dB to 7 dB. In general, the shadowing increases when the height of the TX and/or the RX decreases. This can be explained as follows. With high h_{TX} and h_{RX}, the transmitter and the receiver are in LOS condition and just a part of the power is shadowed by the cow body (e.g., 1 dB for $h_{TX} = 4.5$ m and $h_{RX} = 2$ m, Table 4). However for low h_{TX} and h_{RX}, the communication is totally obscured by the cow body (e.g., 7.4 dB for $h_{TX} = 2$ m and $h_{RX} = 0.5$ m). This validates the result obtained in Section 4.1.2 ($h_{TX} = 1$ m and $h_{RX} = 4.5$ m), where the body of the cow wearing the node was the main reason of the path loss decrease and the other cows had less influence (0.5 dB).

4.3 Temporal fading

4.3.1 Rician K-factor

Fig. 10 shows a typical temporal fading measurement of received power (around median) in dB over time in min, executed in indoor (a) and outdoor (b) environments. Deep fades of 15 dB (15 dB below the median power) occurred several times in the barn (indoor) between 6 and 8 min, as indicated by the red ellipses in Fig. 10. However, this occurred only once on the pasture at the instant t=3 min. This indicates that there are more fading events in barns compared to pastures especially when the cows come close to the antennas. The deep fades all have a short duration, which would very unlikely substantially impair communication between cow nodes and access points.

For each environment, the Rician K-factor is estimated based on the moment method presented in Section 3.2. This method estimates the K-factor directly from the measured samples without need for a curve fitting operation. A K-factor of 10 dB was obtained in the barn and 13 dB in the pasture. These large values indicate a strong specular path LOS component in our measurements due to the TX height (4.5 m). The barn (indoor) K-factor (K=10) is lower than for pasture (K=13), meaning that the contribution of multipath propagation is higher inside the barns in comparison to the pasture.

4.3.2 Cumulative distribution function

The probability that the received power does not exceed a given threshold is determined by the integration of the PDF and is called cumulative distribution function (CDF). Fig. 11-a shows the measured and the analytical (Rice) CDF for the two investigated environments. As shown in this figure, the CDFs in the considered barns and pastures environments follow a Rician distribution.

4.3.3 Fade margin

The obtained K-factors (Section 4.3.1) and the corresponding CDFs (Section 4.3.2) are used to calculate a fade margin associated with temporal fading for a given outage probability. The outage probability, which determines the probability that the wireless system will be out of the service (quality of service not reached) and the corresponding fade margin will be used in the link budget calculation for the network planning application of Section 5.

The details of the calculation are explained in (Andreas, 2011). Fig. 11-b shows the outage probability versus the fade margin in dB. For an outage probability of 0.01 (99% of the time, the variation around the median will not exceed the fade margin), a fade margin of 4 dB in pastures and 6 dB in barns should be considered in the link budget analysis.

5. Application: Network planning

The primary goal of network planning is to provide connectivity, or in other words coverage at all desired locations. Wireless connectivity is determined by a number of parameters such as wireless channel characteristics, the number of receiving nodes, their locations, and the effective isotropic radiated power (EIRP) of the sensor nodes.

In this Section, a ZigBee-based WSN is proposed for the healthcare monitoring of dairy cows. In this network, the on-cow sensor nodes are considered as end nodes and the ZigBee sinks as coordinators. The results and models presented above (Section 4) and the CC2420 chip specifications (CC2420 Datasheet, Texas Instruments 2013) are used to predict and optimise the number of sinks, their locations and power, and the EIRP of the on-cow nodes inside the barns, based on the WiCa Heuristic Indoor Propagation Prediction (WHIPP) tool (Plets et al., 2012). This tool has proven its use for the accurate coverage prediction and optimisation in indoor environments and for optimal network planning.

5.1 Planning tool

The WHIPP tool uses a heuristic planning algorithm, developed and validated for the prediction and optimisation of wireless coverage in indoor environments. The tool is constructed as a web service, which allows importing an existing floor plan in different formats or drawing a floor plan of a building, where the user can choose between different wall materials. The web service transfers this floor plan to a Java backend, after which the server predicts throughput and path loss, based on the path loss model entered by the user. The drawing tool then superimposes this output over the floor plan with a colour code. This gives the user a clear view on the estimated wireless connection quality (coverage) in each area (Plets et al., 2010).

5.2 Planning parameters

After importing the ground plan of the barns, the network parameters and requirements should be defined carefully for an accurate network planning. Table 5 summarises the parameters used for the calculations. Like in the measurements, the transmitter and receiver antenna heights were set to 4.5 m and 1.0 m, respectively. A data rate of 250 kbps was used, which corresponds to the maximum physical data rate of the ZigBee mote (Road and Minnetonka, 2009). The path loss model obtained inside the barns with 15 cows is considered (Table 5). The shadowing margin is determined such that 95% of the locations inside the barn are covered by the wireless system. This margin is derived from the standard deviation σ around the path loss model (Section 4.4.1) and equals 1.65σ. The fade margin obtained inside the barns is considered (See Fig 11-b). All relevant parameters are listed in Table 5.

5.3 Required on-cow node EIRP

The procedure to determine the minimum EIRP required for the uplink (on-cow sensor to sink) wireless connection is presented in Fig. 12. First, the WHIPP tool is used to determine the optimal number and location of the sinks inside the barns given the ground plan of the barn, the base station EIRP, the node's sensitivity, and the path loss model parameters (Section 4.1.1). Based on the optimal placement of the sinks, the maximal path loss between a base station and an on-cow node is determined by the tool. The minimum EIRP required for the uplink connection (sensor node's EIRP) is derived from the maximal path loss and the sensitivity of the sink (base station).

The required number of base stations inside the barn 1 was 1, 2, or 3, depending on the EIRP of the base station. However, barns 2 and 3 have smaller dimensions in comparison to barn 1. Therefore, the required number of base stations was always one (independent of the coordinator's EIRP). Fig. 13 shows the optimal design of the base station network for the three barns (case of two base stations in barn 1). The colour scale illustrates the path loss values between each location and the nearest base station. This maximal path loss value is used to derive the minimally required on-cow node EIRP $\left(EIRP_{node}^{min}\right)$ as follows:

$$EIRP_{node}^{min} = P_{sens}^{BS} + PL_{max} + M_F + M_{Sh} \tag{7}$$

where P_{sens}^{BS} is the base station sensitivity [dBm], PL_{max} the maximal path loss [dB], M_F the fade margin [dB], and M_{Sh} the shadowing margin [dB]. Table 6 lists the minimally required on-cow EIRP for the three investigated barns for different sizes of the base station set. The calculations were performed using the specifications of CC2420 chip (CC2420 Datasheet, Texas Instruments 2013). For barn 1, the sensor node's required EIRP varies between -9.5 dBm and -0.4 dBm depending on the number of base stations, which is related to their EIRP. As this EIRP increases, the required number of base stations decreases and the maximal path loss increases. Thus, the sensor node's EIRP has to increase to maintain a connection. The obtained on-cow node EIRPs for barn 2 and barn 3 were -6.7 dBm and -7.0

dBm, respectively. These values are lower than the transmit power provided by the specifications (Zigbee Alliance, 2011), which means that power consumption reduction can be achieved to increase the battery lifetime of the sensor node (Section 5.5). We note that the number of cows that can be served inside each barn depends on many parameters such as the access method (MAC layer), data load, number of base stations, and the nature of the data to be transferred (critical or non-critical). For example, critical data requires rapid intervention of the farmer and thus real-time updating is required. An on-cow node is covered by the wireless network if its transmitted signal reaches the base station antenna with a power higher than the base station sensitivity. As shown in Table 6, the maximal path loss is lower than 84 dB inside the three barns. Considering an $EIRP_{node}$ of 3 dBm, a base station sensitivity of -95 dBm, a fade margin of 6 dB (Fig. 11-b), and a shadowing margin of 5 dB (see Table 5), then, a path loss PL of 84 dB indicates that this location is covered. Therefore, the three barns are indeed totally covered.

5.4 Power consumption analysis and battery lifetime of sensor node

One of the key factors in determining the success of a WSN is the battery lifetime of the sensor nodes. Since the battery of the sensor node is a limited resource in any WSN, an accurate network planning should optimize the power consumption in order to make the network operational as long as possible. The battery lifetime in hours of the sensor node is estimated as a function of the battery capacity in mAh and the node's activity (awake and sleep periods) as follows:

$$Battery\ lifetime = \frac{Battery\ capacity}{\left(I_{awake}.T_{awake} + I_{sleep}.T_{sleep}\right)}\left(T_{awake} + T_{sleep}\right) \quad (8)$$

where I_{awake} and I_{sleep} are the current consumptions in mA of the sensor node during the awake period T_{awake} (transmitting or receiving data) and the sleep period T_{sleep}in seconds, respectively. The battery lifetime was calculated based on the current consumption of CC2420 chip. According to (CC2420 Datasheet Texas Instruments 2013), I_{awake} varies between 8.5 mA (for -25 dBm transmit power) and 17.4 mA (for 0 dBm transmit power). During the sleep period, the CC2420 chip consumes $I_{sleep} = 0.002$ mA. The total period $T_{period} = T_{awake} + T_{sleep}$ can be configured depending on the WSN application. In our calculations, a realistic value of 1 second for T_{period} was used. Like in (Kwong et al., 2012), battery capacities between 1000 mAh and 5000 mAh were investigated.

Fig. 14 shows an example of calculation of the battery lifetime as a function of the battery capacity for different awake periods when $I_{awake} = 17.4$ mA (0 dBm transmit power). The percentage values indicate the ratio T_{awake}/T_{period}. The battery lifetime increases as the capacity increases. Also, the battery lifetime increases as the awake period decreases. The awake period determines the amount of data that can be transmitted per time unit (1 second). For $T_{awake} = 5$ ms and a throughput of 250 kbps, 1250 bits can be transmitted every second. In this situation, a battery capacity of about 3000 mAh results in a lifetime of about three years. This is an acceptable lifetime, considering the average lifetime of a cow (5 years) and the fact that most cows' anomalies (e.g., mastitis, heat, lameness) occur after the first calving (around second year).Therefore, the cows can be equipped with the healthcare monitoring system during three years.

To estimate the battery lifetime of the on-cow nodes for the three investigated barns, the obtained on-cow EIRP (Section 5.4) are considered with a typical battery capacity of 3000 mAh (Kwong et al., 2012). Since the transmit power of the CC2420 chip varies between -25 dBm and 0 dBm with a step of 5 dBm, each on-cow EIRP (Table 6) is related to the required output power level. Table 7 lists the obtained battery lifetimes for a varying node activity (awake period). In fact, there is a trade-off between the battery lifetime and the node activity. As the activity increases, which is related to the network applications, the battery lifetime decreases. If the data load required for each cow is determined (this depends on the monitored parameters e.g., cow movement, temperature, drinking and eating time), Table 7 can be used then to estimate the battery lifetime for a given on-cow EIRP.
In case of applications that require more throughput, the awake period should be higher, decreasing the battery lifetime. In such situations, wireless charging of the nodes using an inductive powering system (Thoen and Stevens, 2015) can be used to avoid a costly and labour intensive battery

replacement procedure. The inductive powering elements can be installed at the drinking places, so that during the time slots when the cow is drinking the power can be wirelessly transferred to the node's battery. Finally, we note that the battery lifetime calculation presented in this paper provides an estimation depending upon the considered battery technology, connected peripherals, and required duty cycles for each particular application.

6. Conclusions and future work

The off-body wireless channel between a node placed on the body of a dairy cow and an access point inside barns and on pastures has been characterised at 2.4 GHz. The reliability of this wireless connection is a key factor for the success of a cow healthcare monitoring system that facilitates herd management and cow welfare. Three different barns and a pasture have been investigated. Measurements of large-scale fading, cow body shadowing, and temporal fading have been performed with spectrum analysis and ZigBee motes equipment. Results have shown that the large-scale fading can be well described by a one-slope log-normal path loss model. In line-of-sight conditions, the highest path loss increase resulted from the body of the cow wearing the sensor node (3 dB). However, the other cows had less influence (0.5 dB). A cow body shadowing between 1 dB and 7 dB was obtained, depending on the transmitter and receiver heights. The temporal fading was statistically described by Rician distributions. The fading occurrences and depth were higher inside the barns than on the pasture. Consequently, the fade margins were 6 dB and 4 dB for the barns and pasture, respectively. The obtained wireless channel characteristics were then used to optimise the number of the base stations, their EIRP, and their locations inside the investigated barns, based on the WHIPP prediction tool. Assuming typical specifications for the sensor nodes, different network designs were proposed, each with a different impact on the minimal on-cow node transmit power and lifetime. The battery lifetime of the sensor nodes was estimated as a function of the battery capacity, the network design, and the sensor's activity. Battery lifetimes between 143 and 2193 days were obtained depending on the network design and application.

As future research topic, multiple health parameters will be collected from different parts of the cow's body. For example, data from legs, ear, and udder can be transferred to a data collector placed on the cow's neck and then forwarded to the access point. Therefore, future work will investigate the on-body wireless communication between two nodes placed on the cow's body (e.g., leg to neck, udder to neck, and ear to neck).

7. Acknowledgments

This work was supported by the iMinds-MoniCow project, co-funded by iMinds, a research institute founded by the Flemish Government in 2004, and the involved companies and institutions. E. Tanghe is a Post-Doctoral Fellow of the FWO-V (Research Foundation-Flanders). The authors would like to thank Thijs Decroos, Sara Van Lembergen, and Matthias Van den Bossche for their help during the measurements. The authors would like to thank also ILVO and UGent- Biocentrum Agrivet for providing the barns for the measurements.

8. References

Abdi, A., Tepedelenlioglu, C., Kaveh, M., Giannakis, G., 2001. On the estimation of the K parameter for the rice fading distribution. IEEE Commun. Lett. 5, 92–94. doi:10.1109/4234.913150

Akyildiz, I., Su, W., Sankarasubramaniam, Y., Cayirci, E., 2002. Wireless sensor networks: a survey. Comput. Networks 38, 393–422. doi:10.1016/S1389-1286(01)00302-4

Alemdar, H., Ersoy, C., 2010. Wireless sensor networks for healthcare: A survey. Comput. Networks 54, 2688–2710. doi:10.1016/j.comnet.2010.05.003

Andonovic, I., Michie, W., Gilroy, M.P., Goh, H.G., Kwong, K., Sasloglou, K., Wu, T.-T., 2010. Wireless sensor networks for cattle health monitoring. Online 84–89. doi:10.1109/MOBIQUITOUS.2005.65

Andreas, M.F., 2011. Wireless Communications, second. ed, Wiley Publishing. doi:10.1002/9781119992806.fmatter

Balanis, C.A., 2005. Antenna theory: Analysis and design, 3rd ed, Wiley.

Barkema, H.W., Westrik, J.D., van Keulen, K.A.S., Schukken, Y.H., Brand, A., 1994. The effects of lameness on reproductive performance, milk production and culling in Dutch dairy farms. Prev. Vet. Med. doi:10.1016/0167-5877(94)90058-2

Bernadó, L., Zemen, T., Member, S., Tufvesson, F., Member, S., Molisch, A.F., Mecklenbräuker, C.F., Member, S., 2015. Time- and Frequency-Varying K -Factor of Non-Stationary Vehicular Channels for Safety-Relevant Scenarios. IEEE Trans. Intell. Transp. Syst. 16, 1007–1017.

CC2420 Datasheet Texas Instruments 2013, n.d. 2.4 GHz IEEE 802.15.4 / ZigBee-ready RF Transceiver, downloadable at www.chipcon.com.

Huircán, J.I., Muñoz, C., Young, H., Von Dossow, L., Bustos, J., Vivallo, G., Toneatti, M., 2010. ZigBee-based wireless sensor network localization for cattle monitoring in grazing fields. Comput. Electron. Agric. 74, 258–264. doi:10.1016/j.compag.2010.08.014

Kahn, J.M., Katz, R.H., Pister, K.S.J., 2000. Emerging Challenges: Mobile Networking for Smart Dust. J. Commun. Networks 2, 188–196.

Kwong, K.H., Andonovic, I., Wu, T.-T., Goh, H.G., Sasloglou, K., Stephen, B., Glover, I., Shen, C., Du, W., Michie, C., 2012. Practical considerations for wireless sensor networks in cattle monitoring applications. Comput. Electron. Agric. 81, 33–44. doi:10.1016/j.compag.2011.10.013

Lee, W.C.Y., 1985. Estimate of local average power of a mobile radio signal. IEEE Trans. Veh. Technol. 34. doi:10.1109/T-VT.1985.24030

Mayer, K., Ellis, K., Taylor, K., 2004. Cattle health monitoring using wireless sensor networks.pdf.

Nadimi, E.S., Jørgensen, R.N., Blanes-Vidal, V., Christensen, S., 2012. Monitoring and classifying animal behavior using ZigBee-based mobile ad hoc wireless sensor networks and artificial neural networks. Comput. Electron. Agric. 82, 44–54. doi:10.1016/j.compag.2011.12.008

Nadimi, E.S., Søgaard, H.T., Bak, T., Oudshoorn, F.W., 2008. ZigBee-based wireless sensor networks for monitoring animal presence and pasture time in a strip of new grass. Comput. Electron. Agric. 61, 79–87. doi:10.1016/j.compag.2007.09.010

Parsons, J.D., 2000. The Mobile Radio Propagation Channel, Electrical Engineering. doi:10.1049/ir:19920094

Pérez Fontán, F., Mariño Espiñeira, P., 2008. Modelling the Wireless Propagation Channel: A Simulation Approach with MATLAB, Modelling the Wireless Propagation Channel: A Simulation Approach with MATLAB. doi:10.1002/9780470751749

Plets, D., Joseph, W., Vanhecke, K., Tanghe, E., Martens, L., 2012. Coverage prediction and optimization algorithms for indoor environments. EURASIP J. Wirel. Commun. Netw. doi:10.1186/1687-1499-2012-123

Plets, D., Joseph, W., Vanhecke, K., Tanghe, E., Martens, L., 2010. Development of an accurate tool for path loss and coverage prediction in indoor environments. Antennas Propag. (EuCAP), 2010 Proc. Fourth Eur. Conf. doi:10.1109/EUCAP.2010.5505545

Rappaport, T.S., 2002. Wireless communications : principles and practice, Prentice Hall communications engineering and emerging technologies series.

Road, B., Minnetonka, E., 2009. XBee®/XBee-PRO® ZB RF Modules.

Tanghe, E., Joseph, W., Verloock, L., Martens, L., Capoen, H., Van Herwegen, K., Vantomme, W., 2008. The industrial indoor channel: Large-scale and temporal fading at 900, 2400, and 5200 MHz. IEEE Trans. Wirel. Commun. 7, 2740–2751. doi:10.1109/TWC.2008.070143

Thoen, B., Stevens, N., 2015. Development of a Communication Scheme for Wireless Power Applications With Moving Receivers. IEEE Trans. Microw. Theory Tech. 63, 857–863. doi:10.1109/TMTT.2015.2397442

Wang, D., Song, L., Kong, X., Zhang, Z., 2012. Near-ground path loss measurements and modeling for wireless sensor networks at 2.4 GHz. Int. J. Distrib. Sens. Networks 2012. doi:10.1155/2012/969712

Wietrzyk, B., Radenkovic, M., 2010. Realistic Large Scale ad hoc Animal Monitoring. Int. J. Adv. Life Sci. 2, 1–17.

Wilk, M.B., Gnanadesikan, R., 1968. Probability plotting methods for the analysis of data. Biometrika 55, 1–17. doi:10.1093/biomet/55.1.1

Zigbee Alliance, 2011. ZigBee/IEEE 802.15.4 specification.

9. Figure captions

Fig. 1. Indoor and outdoor measurement environments. Indoor (barns (a), (c) and (d) and outdoor (pasture (b)).

Fig. 2. Measurement equpment used for empty barns and pasture (scenario 1). Transmitter side (a) and receiver side (b).

Fig. 3. Measurement setup of the second scenario: environment with cows and setup with ZigBee mots.

Fig. 4. Measurement setup of the cow body shadowing and TX-RX antenna heights investigated.

Fig. 5. RSSI calibration measurements: scenario 1 (a) and scenario 2 (b).

Fig. 6. Measured path loss and fitted models versus distance (Tx-Rx separation) obtained during RSSI calibration (SG signal generator and SA spectrum analyser). The markers indicate the measured samples while the lines indicate the fitted models

Fig. 7. Measured path loss and fitted models versus distance (Tx-Rx separation) for the indoor (barns) measurements.

Fig. 8. Measured path loss and fitted models versus Log-distance (Tx-Rx separation) for the outdoor (pasture) measurements.

Fig 9. QQ plot of Residual path loss versus Standard Normal Distribution for indoor (a) and outdoor (b) environments.

Fig. 10. Typical measurement of temporal fading in indoor (a) and outdoor (b) environments (red ellipses indicate deep fades lower than 15 dB).

Fig. 11. Measured and analytical (Rice) CDFs for indoor (barn) and outdoor (pasture) environments (a). Outage Probability versus fade margin (b).

Fig. 12. EIRP calculation procedure.

Fig. 13. The optimal number of base stations (BS) and thier optimal locations inside the barns (two base stations in barn 1). Color scale shows the path loss values.

Fig. 14. Battery lifetime vesus battery capacity for different awake periods in a time frame T_{period} of one second ($CC2420$: $I_{awake} = 17$ mA and $I_{sleep} = 0.002$ mA)

10. Table captions

Table 1. Parameter values of the path loss models.

	$d_0[m]$	$PL(d_0)\ [dB]$	$n[-]$	$\sigma[dB]$	$R^2[-]$
ZigBee-ZigBee	1	49	1.60	3.5	0.74
ZigBee- Spectrum analyser	1	41.2	1.80	3.1	0.80
Signal generator - Spectrum analyser	1	41.7	1.70	4.0	0.70

Table 2. Parameter values of the path loss models indoor (barns).

	$d_0[m]$	$PL(d_0)\ [dB]$	$n[-]$	$\sigma[dB]$	$R^2[-]$
Barn 1 empty	1	48.0	1.50	3.7	0.70
Barn 2 emty	1	49.8	1.58	3.8	0.78
Barn 3 empty	1	47.0	1.51	3.28	0.82
Barns empty	1	48.6	1.50	3.7	0.8
Barn 1 with 15 cows	1	52.4	1.68	2.8	0.82

Table 3. Parameter values of the path loss models outdoor (pasture).

	$d_0[m]$	$PL(d_0)\ [dB]$	$n[-]$	$\sigma[dB]$	$R^2[-]$
Empty pasture	1	39.5	2.18	3.8	0.73
Pasture with one cow	1	42.8	2.25	2.6	0.81
Pasture with 8 cows	1	42.4	2.3	5.3	0.71

Table 4. Values of the cow body shadowing.

Shadowing [dB]		h_{TX}[m]	
		2	4.5
h_{RX}[m]	0.5	7.4	4.0
	1	3.7	3.1
	1.4	2.8	2.4
	2	1.0	1.0

Table 5. Parameters used for network planning.

	Parameters	Value	Unit
Coordinator (base station)	Throughput	0.250	Mbps
	Sensitivity	-95*	dBm
	Elevation	4.5	m
Margins	Interference margin	0	dB
	Shadowing margin (95 %)	5	dB
	Fade margin	6	dB
Path loss model	Reference distance	1	m
	Reference path loss	52.4	dB
	Path loss exponent	1.7	[-]
End nodes (sensor nodes)	Throughput	0.250	Mbps
	Sensitivity	-95	dBm
	Elevation	1	m

* CC2420 Datasheet, Texas Instruments, March 2013. Downloadable at www.chipcon.com

Table 6. Minimum on-cow node EIRP for the three investigated barns.

Base station EIRP [dBm]	Barn	Number of required base stations	Maximal path loss [dB]	Minimally required on-cow node EIRP [dBm]
EIRP<0	Barn 1	3	74.5	-9.5
	Barn 2	1	77.3	-6.7
	Barn 3	1	77	-7.0
0<EIRP<5	Barn 1	2	79.5	-4.5
EIRP>5	Barn 1	1	83.6	-0.4

Table 7. Battery lifetime [days] estimation for different on-cow EIRP and awake periods based on cc2420 power consumption and a typical battery capacity of 3000 mA.

Barn (number of base stations BS)	On-cow node EIRP [dBm]	Corresponding CC2420 output power [dBm]	Current Consumption (transmit mode) [mA]	Battery lifetime [days]			
				5 ms (0.5%)	10 ms (1.0%)	20 ms (2.0%)	50 ms (5.0%)
Barn 1 (3 BS)	-9.5	-10	11	2193	1116	563	226
Barn 2 (1 BS)	-6.7	-5	14	1736	880	443	178
Barn 3 (1 BS)	-7.0						
Barn 1 (2 BS)	-4.5						
Barn 1 (1 BS)	-0.4	0	17	1405	710	357	143

11. Figure captions

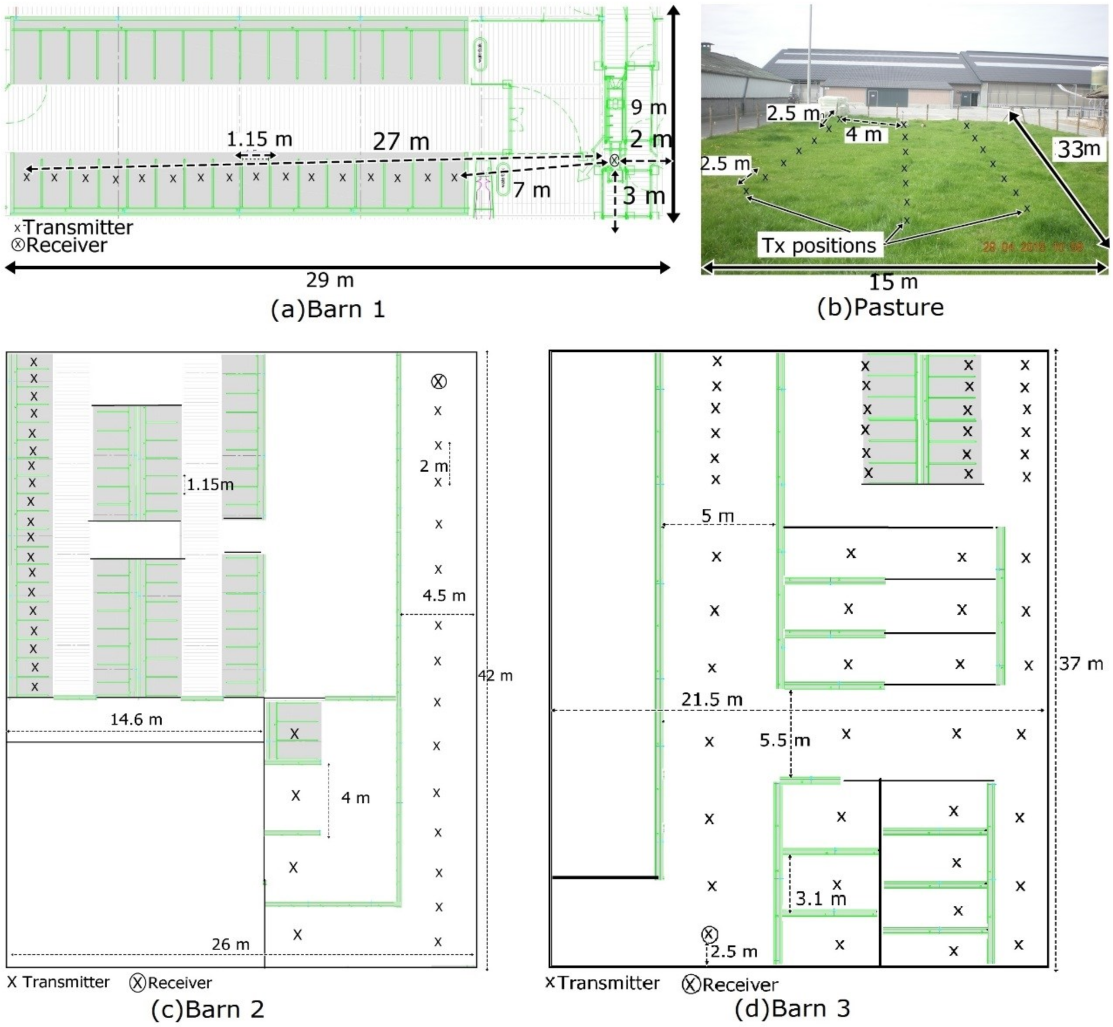

Fig. 1. Indoor and outdoor measurement environments. Indoor (barns (a), (c) and (d) and outdoor (pasture (b)).

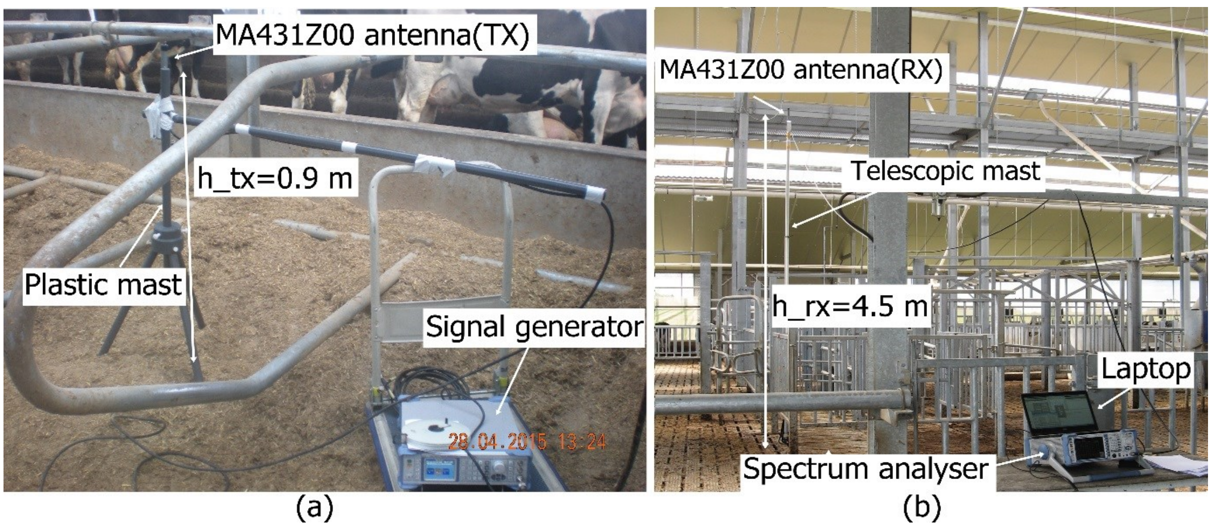

Fig. 2. Measurement equpment used for empty barns and pasture (scenario 1). Transmitter side (a) and receiver side (b).

Fig. 3. Measurement setup of the second scenario: environment with cows and setup with ZigBee mots.

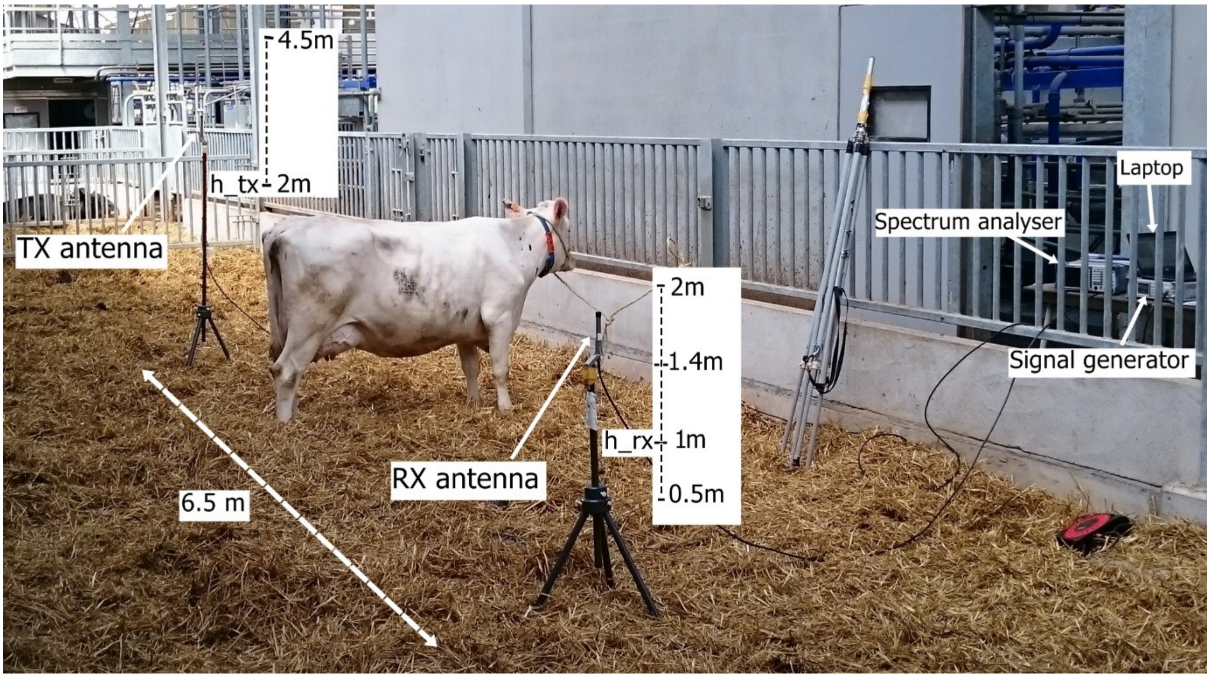

Fig. 4. Measurement setup of the cow body shadowing and TX-RX antenna heights investigated.

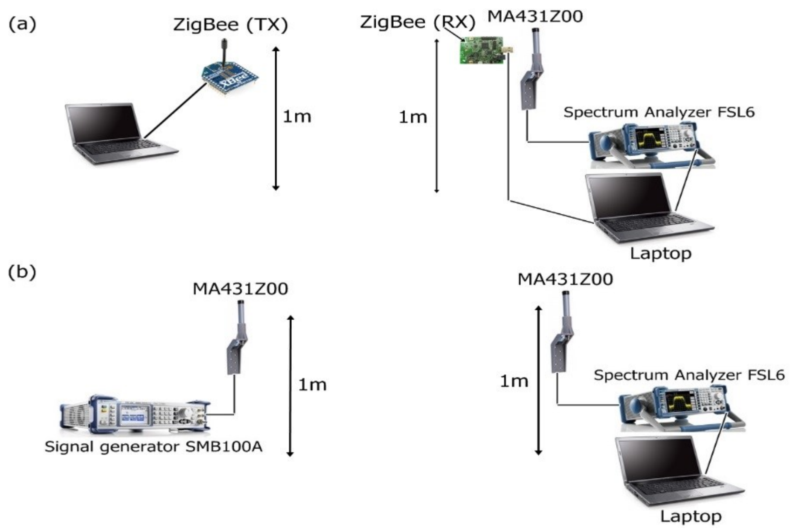

Fig. 5. RSSI calibration measurements: scenario 1 (a) and scenario 2 (b).

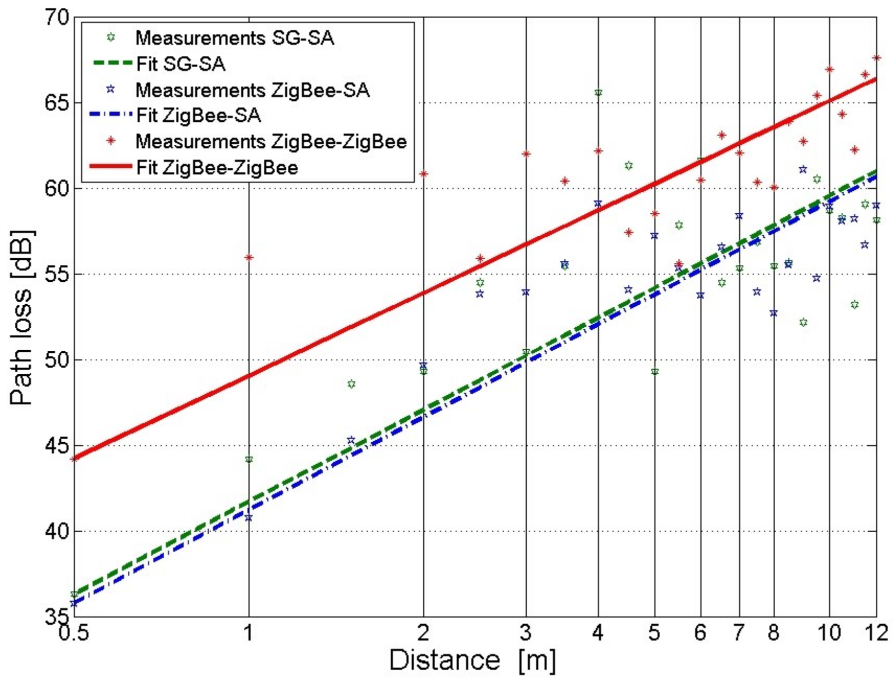

Fig. 6. Measured path loss and fitted models versus distance (Tx-Rx separation) obtained during RSSI calibration (SG signal generator and SA spectrum analyser).

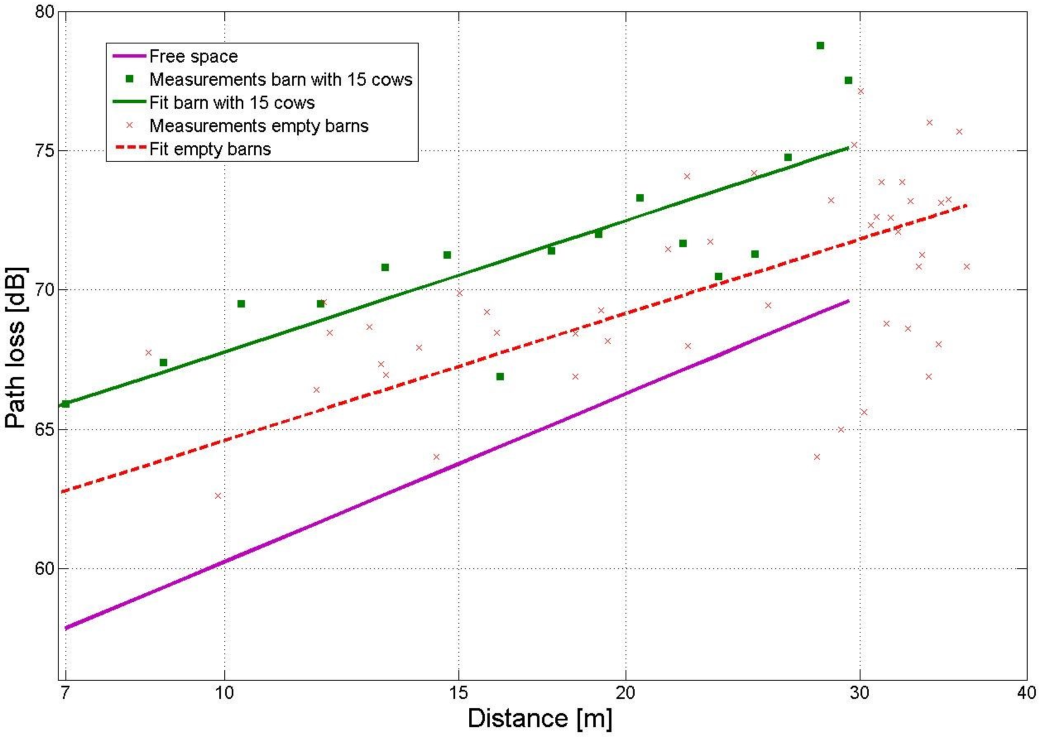

Fig. 7. Measured path loss and fitted models versus distance (Tx-Rx separation) for the indoor (barns) measurements.

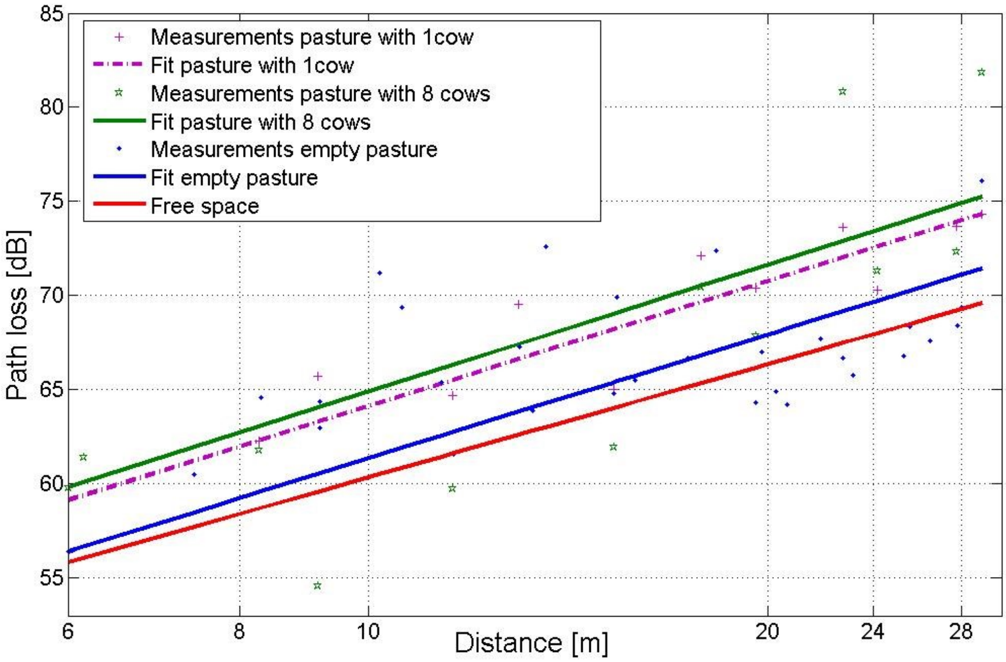

Fig. 8. Measured path loss and fitted models versus Log-distance (Tx-Rx separation) for the outdoor (pasture) measurements.

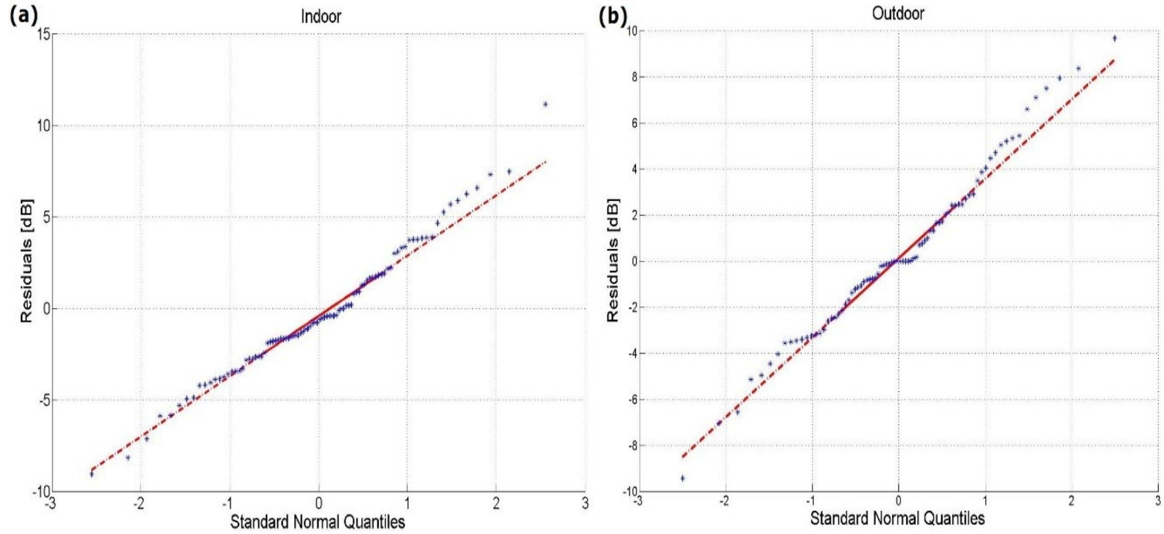

Fig. 9. QQ plot of Residual path loss versus Standard Normal Distribution for indoor (a) and outdoor (b) environments.

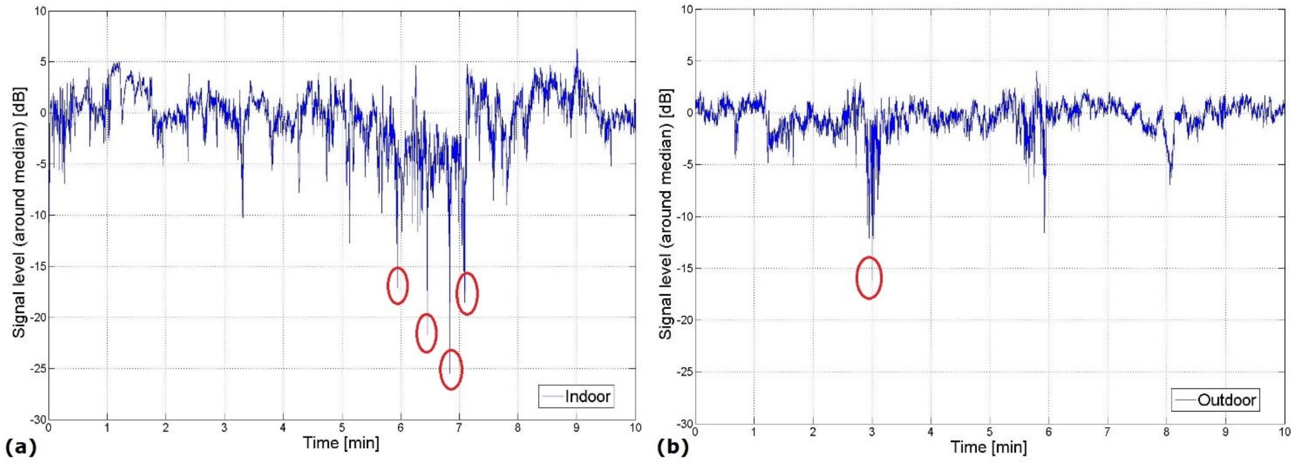

Fig. 10. Typical measurement of temporal fading in indoor (a) and outdoor (b) environments.

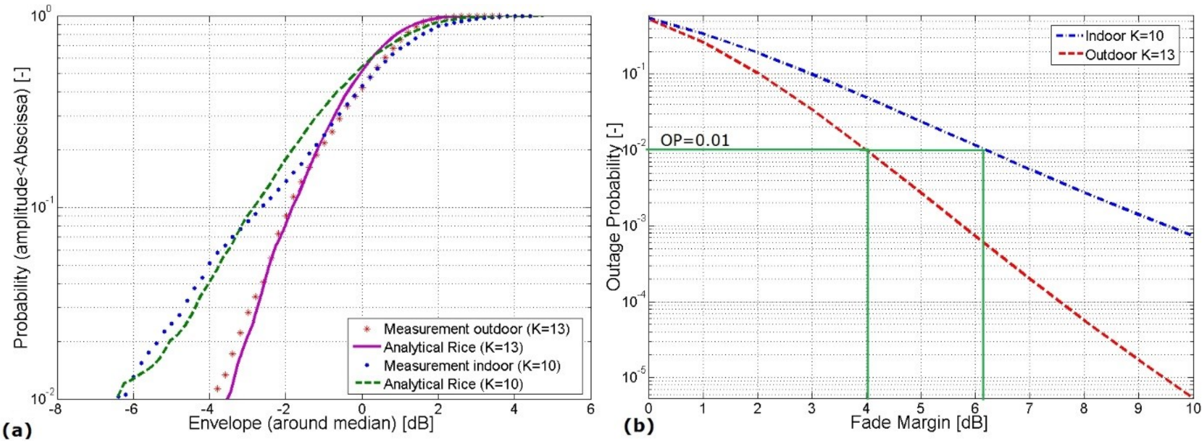

Fig. 11. Measured and analytical (Rice) CDFs for indoor (barns) and outdoor (pasture) environments (a). Outage Probability versus fade margin (b).

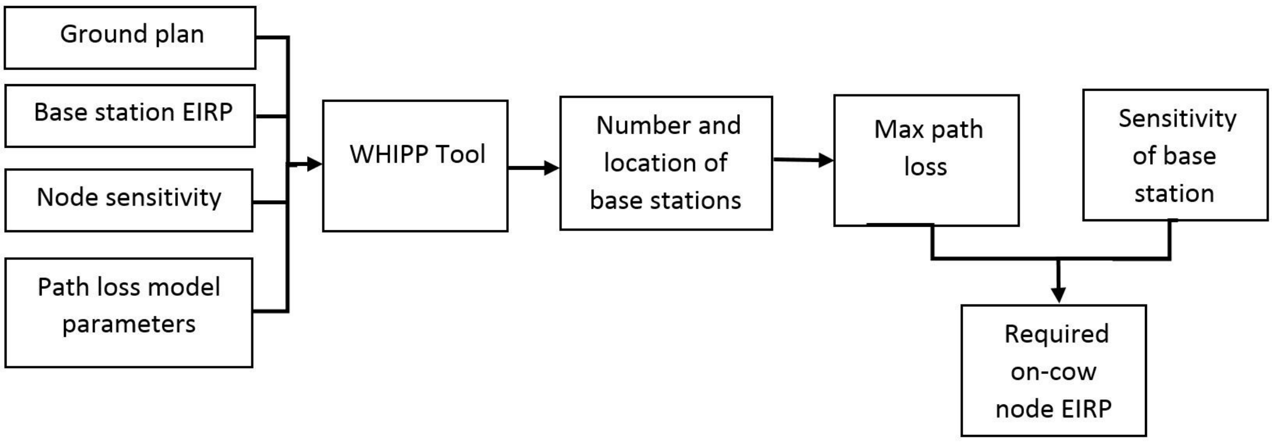

Fig. 12. EIRP calculation procedure.

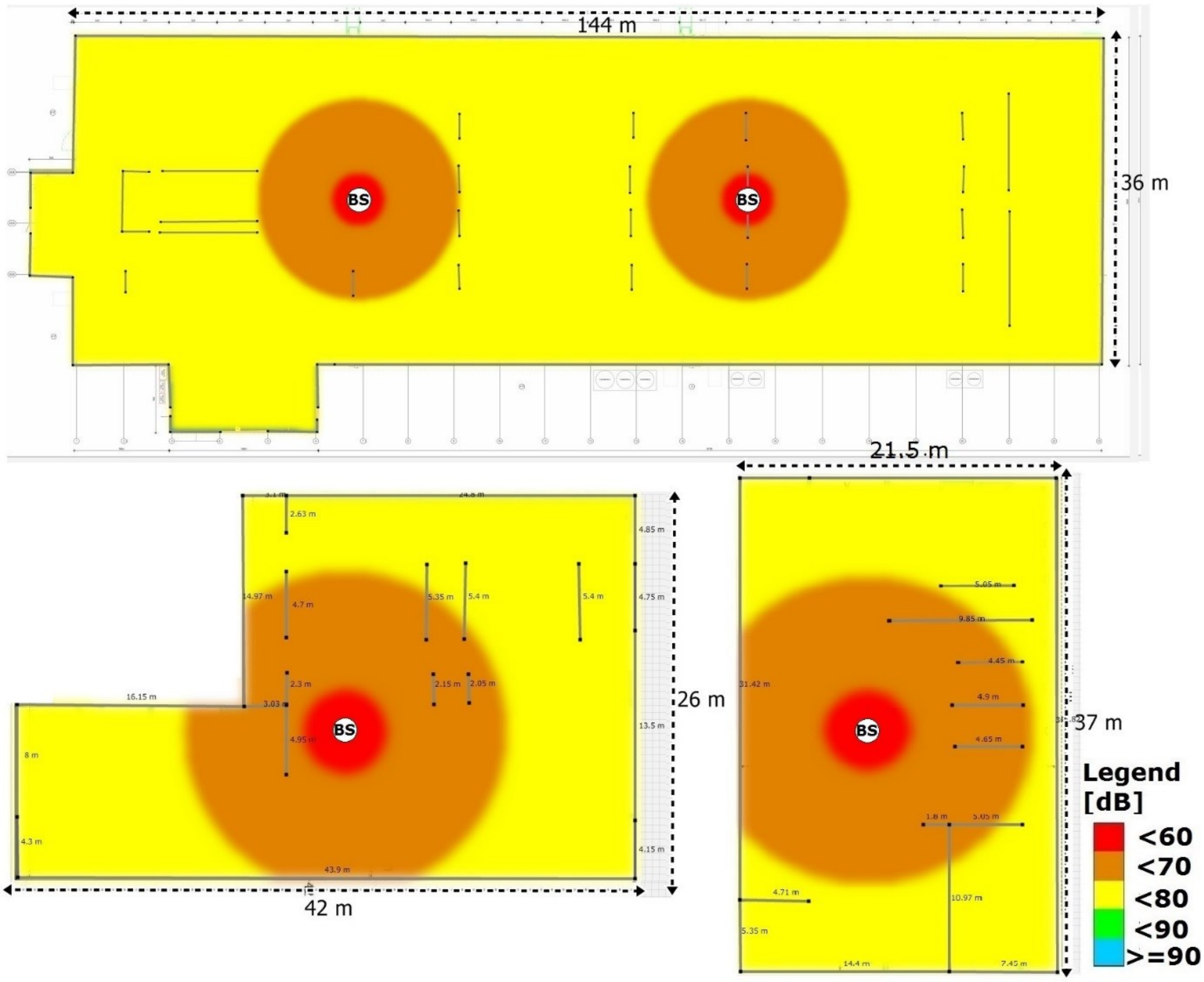

Fig. 13. The optimal number of base stations (BS) and thier optimal locations inside the barns (two base stations in barn 1). Color scale shows the path loss values.

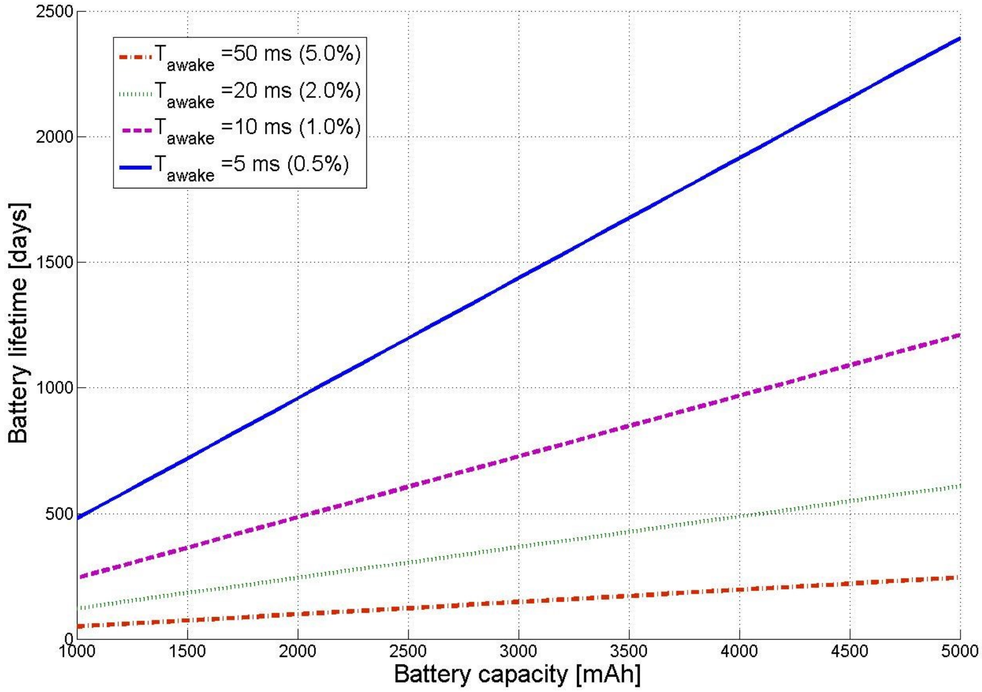

Fig. 14. Battery lifetime vesus battery capacity for different awake periods in a time frame T_{period} of one second ($CC2420$: $I_{awake} = 17$ mA and $I_{sleep} = 0.002$ mA)